Phase separation of a magnetic fluid: Asymptotic states and nonequilibrium kinetics

Anuj Kumar Singh

Working with
Prof. Varsha Banerjee

Department of Physics
Indian Institute of Technology Delhi, New Delhi, India

CompPhys23, Leibzig

December 20, 2023

Introduction

Magnetic colloids:

- Comprise of single-domain magnetic particles dispersed in the carrier liquid.
- Modeled as spherical particles with the inclusion of magnetic moment at their center.
- Anisotropic system with long-range interacting potential.
- Manifestations include **ferrofluids, magnetic fluids, and dipolar fluids**.
- Exhibit a gas-liquid (GL) phase coexistence and magnetic order even in the absence of an external field.
- Form structures in the GL coexistence regime and aggregates easily respond to the magnetic fields.
- Combines the dual characteristics of particles as **fluidity** with the **magnetic order**.
- Widely used in the mixture of **LC+MNP** and an excellent choice for **hybrid material design**.

Interactions in the magnetic colloidal particles

$$U_{LJ} = 4\epsilon \sum_{j,i\neq j} \left[\left(\frac{\sigma}{r_{ij}}\right)^{12} - \left(\frac{\sigma}{r_{ij}}\right)^{6} \right]$$

- **Lennard Jones:** Isotropic and short-range.
  - **First term:** Prevents particles from overlapping.
  - **Second term:** Weak van der Waal's attraction.
    $\rightarrow$ For the aggregation of particles

$$U_{dd} = \frac{\mu_0}{4\pi} \sum_{j,i\neq j} \left[\frac{1}{r_{ij}^3}(\vec{\mu}_i.\vec{\mu}_j) - \frac{3}{r_{ij}^5}(\vec{\mu}_i.\vec{r}_{ij})(\vec{\mu}_j.\vec{r}_{ij}) \right]$$

- U_{dd}: Dipole-dipole interaction.
  - Anisotropic and long-range.
  - Conflicting interaction can be 0 or ± 1 depending on the orientation of μ.
- **Experimentally observed the GL coexistence regime for magnetic colloids system.**
- **SM fluid is the suitable model for the magnetic colloidal system due to its capturing the aggregation of particles and the existence of a GL coexistence phase diagram.**

SM model and phase diagram

- For **SM model** all interactions lies between maximum repulsion and attraction.
  - $\theta = \pi$: Maximum repulsion
  - $\theta = \pi/2$: No dipolar interaction
  - $\theta = 0$: Maximum attraction

- **Isotropic weak van der Waal's attraction** of LJ potential is responsible for the GL phase coexistence.

- Solid red line is **binodal**, while the blue dotted line is **spinodal**.

- Dipole moment μ control the GL coexistence regime and shift the critical temperature T_c and density ρ_c.

- **Spinodal decomposition:** Phase separation by the spontaneous growth of fluctuations.

- **Nucleation and growth:** Free-energy barrier must be overcome for the formation of a nucleus.

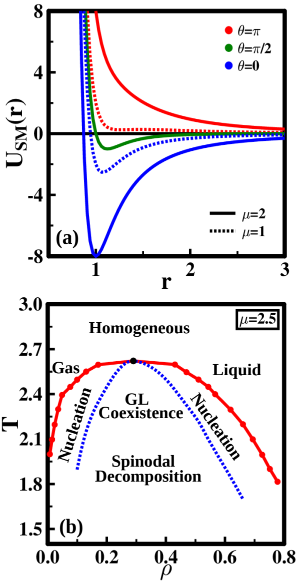

M. J. Stevens and G. S. Grest. Phys. Rev. E, 51 (1995).

Structural phases in coexistence regime

- Quench the system from isotropic state $T=5.0$ to $T=1.05$ for $\rho=0.05[\boldsymbol{Q_n}]$ and $\rho=0.2[\boldsymbol{Q_s}]$

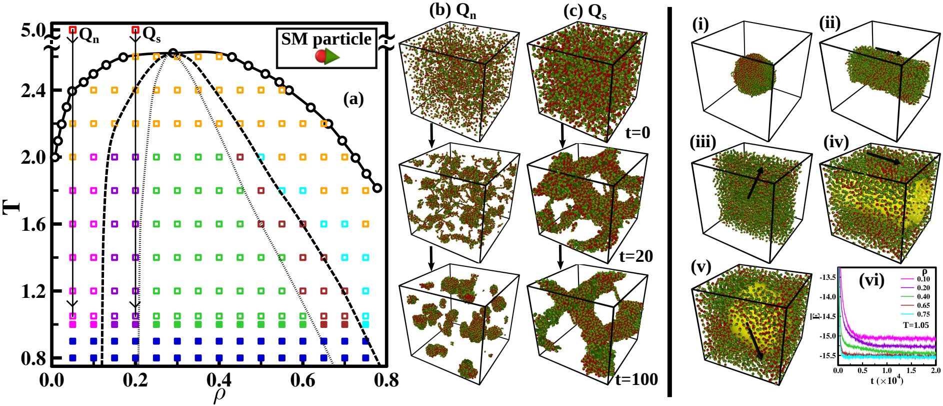

- For $[\boldsymbol{Q_n}]$, discrete morphologies $\rightarrow$ the growth is via nucleation and subsequent consolidation.
- For $[\boldsymbol{Q_s}]$, bi-continuous morphology $\rightarrow$ the growth is via spinodal decomposition.
- The equilibrium structures assume shapes with minimum surface energy.

Coarsening study

Quenching from a high-temperature homogeneous state to the coexistence regime at t=0:

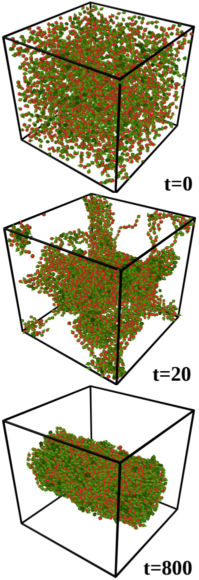

- **Solid systems:**
  - For **conserved kinetics**, *Lifshitz-Slyozov (LS)* growth law: *Binary alloys*, $\ell(t) \sim t^{1/3}$
  - For **non-conserved kinetics**, *Lifshitz-Allen-Cahn* growth law:
    Ising magnets (short-range): $\ell(t) \sim t^{1/2}$
    Dipolar system (long-range): $\ell(t) \sim t$

- **Fluid systems:**
  - Hydrodynamic effects become important after the diffusive regime.
  - **Furukawa** argued that
    At early time: fluid inertia << fluid viscosity
    At late time: fluid inertia >> fluid viscosity

$$\ell(t) \sim \begin{cases} t^1, & \ell \ll \frac{\eta^2}{\tilde{\sigma}\rho} \text{ (viscous hydrodynamics)} \\ t^{2/3}, & \frac{\eta^2}{\tilde{\sigma}\rho} \ll \ell \text{ (inertial hydrodynamics)} \end{cases}$$

  - **Furukawa predicted at late time**, domain growth in binary fluids scales as $\ell(t) \sim t^{2/3}$
  - **The inertial growth has been elusive in MD simulations.**

H. Furukawa, Phys. Rev. A 31, 1103 (1985).

Correlation function and structure factor

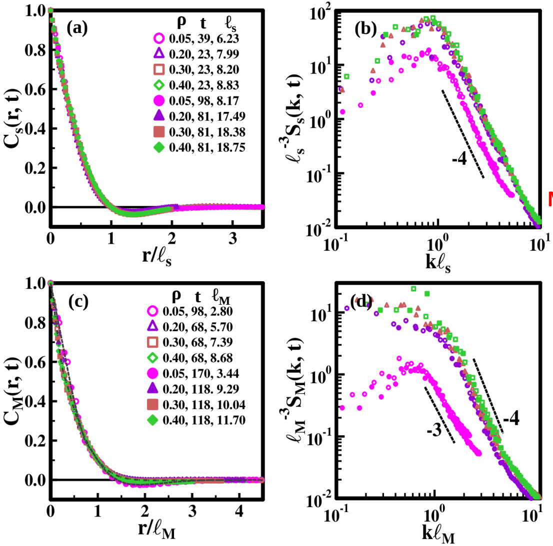

Spatial ordering:

- **Conserved** dynamics.
- $S(k) \sim k^{-(d+1)} \sim k^{-4}$ **(Generalised Porod law)**
- $S(k,t)$ indicating scattering from smooth GL interface.

Magnetic ordering:

- **Spinodal:** Non-conserved dynamics
  - $S(k) \sim k^{-(d+n)} \sim k^{-4}$ **(Generalised Porod law)**
  - Scattering from interface separating spin domains
- **Nucleation:** Conserved dynamics
  - Consistent with our observation of the magnetic Janus sphere.
  - $S_s(k) \sim k^{-3}$; ρ=0.05: Scattering off the 2-d interface for domains of ↑ and ↓ spins.

Accelerated inertial regime in the spinodal regime

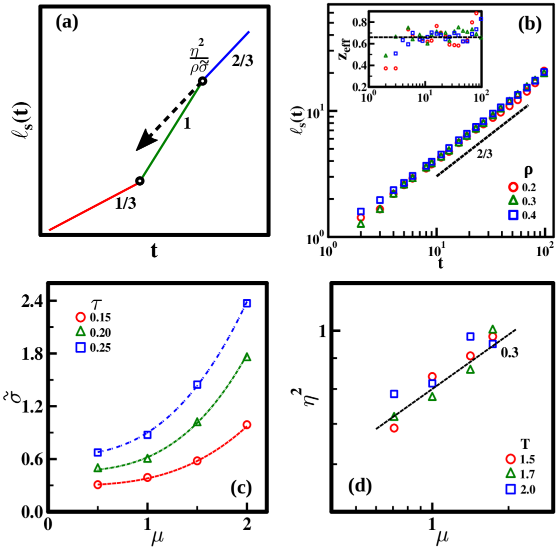

- (a) Graphical representation of diffusive, viscous and inertial regimes
- (b) Accelerated inertial regime: $\ell(t) \sim t^{2/3}$, hitherto never observed in MD simulations.
- (c) $\tilde{\sigma}$ vs. μ for specified values of the reduced temperature τ. $\tilde{\sigma} \approx \tilde{\sigma}_0 + a\mu^3$.

  B. Groh and S. Dietrich, ibid 74, 2617 (1995)
- (d) η^2 vs. μ for $\rho = 0.6$ and specified values of T. $\eta^2 \sim \mu^{0.3}$

  S. Nagy, D. Balogh, and I. Szalai, Fluid Phase Equilib 509 (2020)
- $\frac{\eta^2}{\rho\tilde{\sigma}}$ decreases with μ and accelerates the inertial regime.

Effect of the thermostats, L, ρ, and μ on spatial length scale

- **Nośe-Hoover thermostat (NHT):** $\ell_s(t) \sim t^{2/3}$
  It preserves the relevant feature of hydrodynamics for the study of domain growth.

- **Dissipative particle dynamics (DPD):** $\ell_s(t) \sim t^{2/3}$ It preserves the hydrodynamics mode.

- **Langevin thermostat (LT):** $\ell_s(t) \sim t^{1/3}$ Stochastic nature kills the hydrodynamics mode.

- The range (decade) of spatial growth $\ell_s(t) \sim t^{2/3}$ increases with system size.

- Length scale for nucleation and growth at density $\rho = 0.05$: $\ell_s(t) \sim t^{1/3}$

- For $\mu \gtrsim 1.0$, domain growth exhibit a clear $t^{2/3}$ growth law

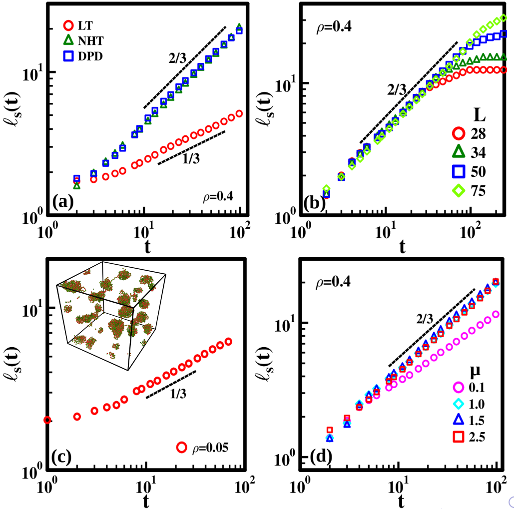

Comparison of growth laws in nucleation and spinodal regime

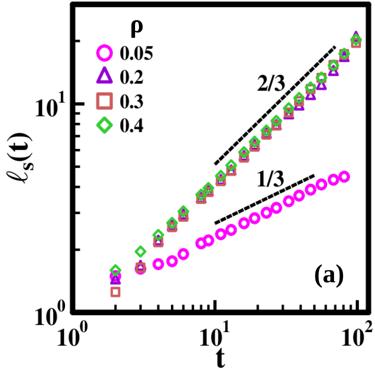

- **Spinodal regime:**
  $\ell_s(t) \sim t^{2/3} \rightarrow$ Accelerated inertial regime
  $\ell_M(t) \sim t^1 \rightarrow$ Growth law consistent with the dipolar solid
- **Nucleation regime:**
  $\ell_s(t) \sim t^{1/3} \rightarrow$ Diffusive regime
  $\ell_M(t) \sim t^{1/3} \rightarrow$ Consistent with the observation of magnetic Janus sphere
- Spatial ordering **triggered** the magnetic ordering.

Physical state of the condensate

PCF:

- $T=2.0$ → gas phase.
- $T=1.05$, → liquid phase.
- For $T=1.0,\ 0.8$, observe several new peaks corresponding to the lattice spacing.

Magnetization M:

- As $T\downarrow$, the dipole-dipole interactions dominate, and $M\uparrow$ due to the formation of chains that co-align parallel to the surface.
- At very low temperatures, $M\downarrow$, presumably due to the freezing of the μ.

MSD:

- At higher $T=\ 2.0,\ 1.05$, the dipoles exhibit ballistic diffusion.
- At lower $T=\ 1.0,\ 0.8$, clear plateau signifying trapping of dipoles.

EA parameter:

- At low T, $q_{EA}\rightarrow 1$ whereas $M\rightarrow 0$ which is a characteristic signature of glassy order.

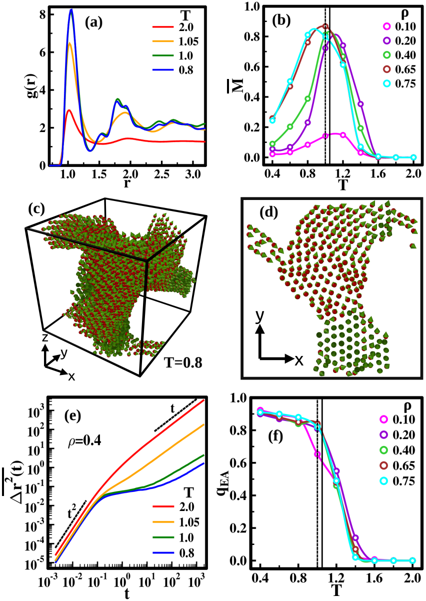

Development of spatial and magnetic order

- **PCF in nucleation:** The peaks are sharper and more in number for the solid phase.
- **PCF in spinodal decomposition:** Sharper peaks are more pronounced in solid state.
- **BOP in liquid:** No local spatial order, although there is magnetic order.
- **BOP in solid:**
  - Isotropic structures do not exhibit crystalline order.
  - Anisotropic structures exhibit crystalline order.
- The anisotropic structures are predominantly FCC crystalline order over the HCP structure.

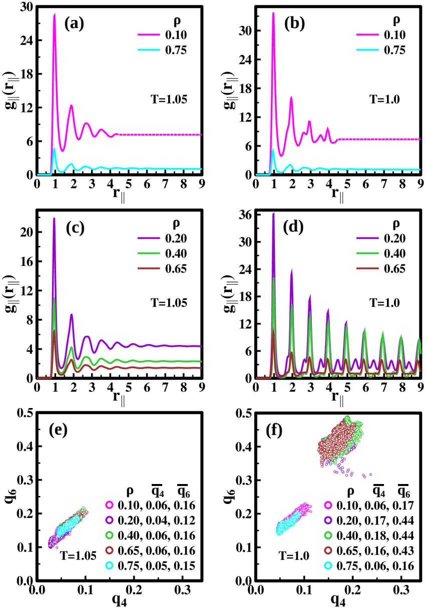

- Magnetic properties develop in the condensates due to the interplay of the surface energy and the dipole-dipole interactions U_{dd}.
- $U_{dd} > k_B T$, μ form long chains that align along the surface.
- We have a magnetic Janus sphere composed of two hemispherical domains with opposite magnetic orientations.
- Magnetic Janus sphere is observes for $\mu \geq 1.5$.

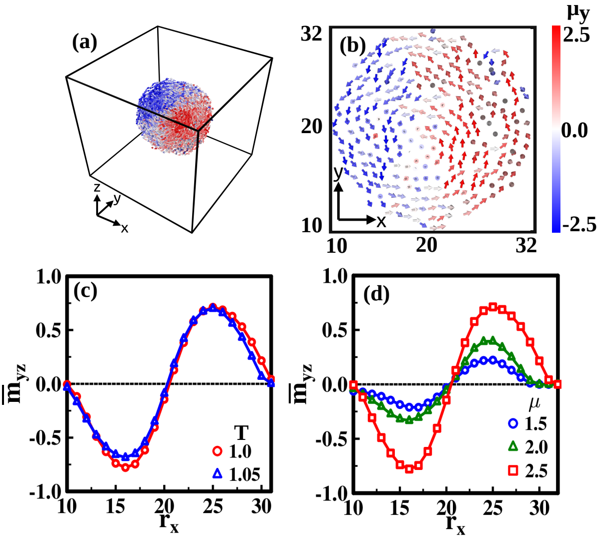

Cross-section of morphologies with magnetic profile

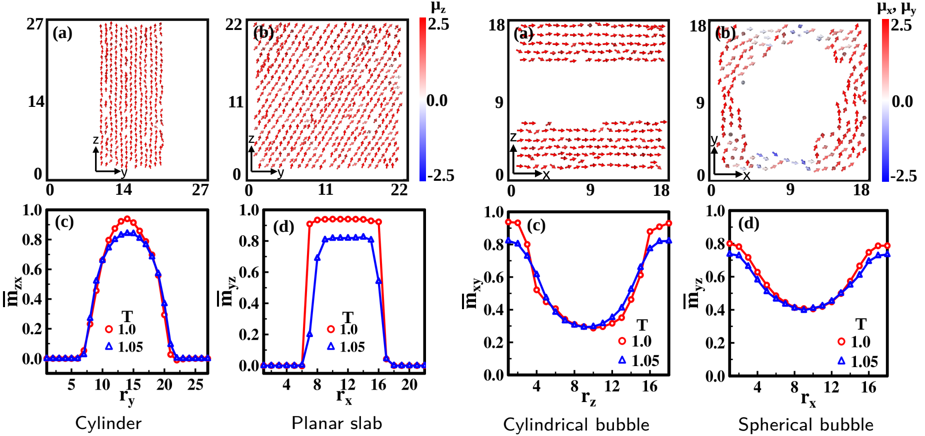

- Cross-sections corresponding to the structural morphologies for $T = 1.0$.
- The moments align along the surface to form long chains.
- The cylinder, planar slab, and cylindrical bubble provide uniformly magnetized self-assemblies.
- The spherical bubble has a large M on the surface, which gradually reduces at the center.

Summary of the Talk

- The coarsening morphologies in the spinodal decomposition are bi-continuous and exhibit an *accelerated inertial growth law* $\ell_s(t) \sim t^{2/3}$, hitherto never observed in MD simulations.

- *Triggered magnetic order* in the liquid phase that grows as $\ell_M(t) \sim t$, typical of dipolar magnets with non-conserved order parameter dynamics.

- The structural phases are density dependent with spatial and magnetic order.
  $\rightarrow$ minimum energy shapes for the corresponding densities.

- The magnetic moments always co-align with the surface.

- The sphere is a magnetic Janus particle due to an oppositely magnetized hemisphere.

- For lower $T \simeq 1.0$, the structures solidify, and exhibit quasi-long-range order.
  $\rightarrow$ predominantly FCC over HCP.

[1] Anuj Kumar Singh and Varsha Banerjee, Soft Matter **19**, 2370 (2023).

[2] Anuj Kumar Singh and Varsha Banerjee, Phys. Rev. E **108**, 064604 (2023).

Thank You

Tools for non-equilibrium morphology characterization

- **Correlation function:** $C(\vec{r}_i, \vec{r}_j, t) = \langle \psi(\vec{r}_i).\psi(\vec{r}_j) \rangle - \langle \psi(\vec{r}_i) \rangle \langle \psi(\vec{r}_j) \rangle$
  - $\psi(\vec{r}_i)$ is an appropriate order paramater.
  - The continuum system is mapped onto a spin-lattice by discretizing the volume V into sub-boxes of size 2^3.
  - Our results do not depend on the size of the sub-boxes.

- **Spatial ordering:** $\psi_s(\vec{r}) = \begin{cases} +1, & \text{if } \rho_r > \rho \text{ (liquid state)} \\ -1, & \text{if } \rho_r < \rho \text{ (gas state)} \end{cases}$
  - ℓ_s: First zero crossing of the spatial correlation function.

- **Magnetic ordering:** $\psi_M(\vec{r}) = \begin{cases} \frac{1}{n} \sum_i \vec{\mu}_i, & \text{if } \rho_r > \rho \text{ (liquid state)} \\ 0, & \text{if } \rho_r < \rho \text{ (gas state)} \end{cases}$
  - $\ell_M = 0.1 \times \max[C(\vec{r}, t)]$

- Small-angle scattering experiments yield the **structure factor**: $S(k) = \int d\vec{r} e^{-i\vec{k}.\vec{r}} C(r)$
  - $\vec{k}$ is the wave-vector of the scattered beam.
  - **Generalised Porod law:** For n-component of order parameter and d-dimensionality, S(k) decays as: $S(k) \sim k^{-(n+d)}$.
  - The tail of the structure factor conveys information about defects within the morphologies.

Characterization tools for asymptotic morphologies

- **Pair correlation function (PCF):**
  - For isotropic system: $g(r) = \frac{1}{N\rho_0}\left\langle \sum_{\substack{i,j \\ i\neq j}}^{N} \frac{\delta(r-r_{ij})}{(4/3)\pi[(r+\Delta r)^3 - r^3]} \right\rangle$
  - For anisotropic system: $g_{\parallel}(r_{\parallel}) = \frac{1}{N\rho_0}\left\langle \sum_{\substack{i,j \\ i\neq j}}^{N} \frac{\delta(r_{\parallel}-r_{ij,\parallel})\theta(\sigma/2-r_{ij,\perp})}{\pi(\sigma/2)^2 h} \right\rangle$
  - Where $r_{ij,\parallel} = |\vec{r}_{ij}.\hat{n}|$, and $r_{ij,\perp} = |\vec{r}_{ij} - (\vec{r}_{ij}.\hat{n})\hat{n}|$

- **Magnetization:** $M = \sum_{i=1}^{N} \vec{\mu}_i / N$
  - $\hat{\mu}_i$ is the dipole moment of the i^{th} particle

- **Mean Square displacement:** $\Delta r^2(t) = \langle (r(t) - r(t_0))^2 \rangle$
  - **At very short time:** $\Delta r^2(t) \sim t^2 \Rightarrow$ Ballistic motion
  - **At very high time:** $\Delta r^2(t) \sim t \Rightarrow$ Diffusive motion
  - **At intermediate time:** Shows plateau region due to the cadging of particles within the local minima

- **Edward Anderson (EA) order parameter:** $q_{EA} = [\langle \mu_i \rangle^2]_{av}$
  - $\langle\rangle$ is the thermal or dynamic average
  - $[]_{av}$ is the ensemble average.
  - Paramagnetic phase: $q_{EA} = 0,\ M = 0$
  - Ferromagnetic phase: $q_{EA} = 0,\ M \neq 0$
  - Glassy phase: $q_{EA} \neq 0,\ M \simeq 0$

Evaluation of local bond order parameter (BOP)

- BOP, q_4 and q_6: For local crystalline order in undercooled liquids and solids.
- Based on spherical harmonics $Y_{lm}(\theta(r_{ij}), \phi(r_{ij}))$.

$$q_l(i) = \sqrt{\frac{4\pi}{2l+1} \sum_{m=-l}^{l} |\bar{q}_{lm}(i)|^2}$$

$$\bar{q}_{lm}(i) = \frac{1}{N_n(i)+1} \sum_{k=0}^{N_n(i)} q_{lm}(k)$$

$$q_{lm}(i) = \frac{1}{N_b(i)} \sum_{j=1}^{N_b(i)} Y_{lm}(r_{ij})$$

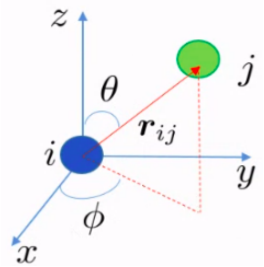

- N_b: number of neighbors (obtained from $g(r_{ij})$).
- Above definition of BOP involves an additional averaging over the second shell of particle i.
- Values of q_4 and q_6 for the perfectly symmetric configurations.

q_l	**simple cubic (SC)**	**body centered cubic (BCC)**	**face centered cubic (FCC)**	**hexagonal close packed (HCP)**
q_4	0.764	0.509	0.190	0.097
q_6	0.354	0.629	0.575	0.484